EXPERIMENTAL AND NUMERICAL INVESTIGATION OF THE SHEAR-DRIVEN FLOW IN A TOROID OF SQUARE CROSS-SECTION

Joseph Humphrey, Joshua Cushner and Ranga Sudarsan
Department of Mechanical and Aerospace Engineering
University of Virginia
Charlottesville, VA 22904, USA
jach@virginia.edu

Mohammad Al-Shannag, Joan Herrero and Francesc Giralt
Department of Chemical Engineering
University of Rovira i Virgili
43006 Tarragona, Catalunya
Spain
fgiralt@etseq.urv.es

ABSTRACT

It is shown that the two-dimensional shear-driven flow in a plane square enclosure is a limiting case of the more general shear-driven flow that can be realized experimentally in a toroid of square cross-section. Visualization and calculations of the flow in a toroid reveal many of the features displayed by sheared fluids in finite-length parallelepipeds, as well as new findings. These include the appearance of Goertler vortices and flow unsteadiness as precursors for laminar to turbulent flow transition, and the occurrence of an oscillatory state of fluid motion not observed in parallelepipeds. Unlike the shear-driven flow in a parallelepiped, that in a toroid is devoid of contaminating end wall effects. Consequently, it represents a more general paradigm in fluid mechanics.

INTRODUCTION

The two-dimensional (2D) shear-driven flow in a plane rectangular enclosure, also referred to as the "lid- or wall-driven cavity flow," has been a computational fluid dynamics paradigm of long-standing interest. Although such a flow has not been rigorously realized in practice, experimental approximations have been achieved in enclosures shaped like parallelepipeds of rectangular cross-section. In the parallelepiped geometry, fluid motion is induced by the in-plane sliding of one of the four longitudinal walls of the parallelepiped in a direction normal to its longitudinal axis.

In the case of the plane square enclosure (Fig. 1-a), the flow is characterized by the Reynolds number $Re = D\,U/\nu$, where D is the characteristic cross-section length, U is the sliding wall velocity, and ν is the kinematic viscosity of the fluid. In the case of a parallelepiped of square cross-section (Fig. 1-b) it is also necessary to specify the longitudinal to cross-section length ratio, L/D. In contrast to the 2D flow in the idealized plane square enclosure, that in a parallelepiped is 3D due to end wall effects, and beyond a critical value of Re because of centrifugal instabilities.

We propose a new geometrical configuration for the investigation of flow instabilities in shear-driven

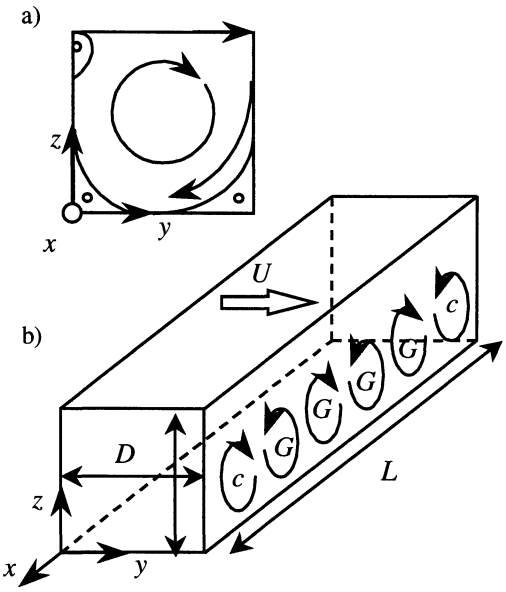

Figure 1. Shear-driven flows in enclosures of square cross-section: a) 2D flow in a plane enclosure; b) 3D flow in a parallelepiped. At sufficiently large Re, centrifugal instabilities trigger Goertler vortices in the parallelepiped where the two end walls fix the sense of rotation of the corner ("c") vortices and, as a consequence, of the remaining ("G") vortices. The sense of rotation of the vortices in the bottom half of the parallelepiped is shown projected on an x-z plane.

enclosures that is realizable experimentally and numerically without incurring the end wall bias present in the finite parallelepiped configuration. This consists of the shear-driven flow in a toroid of square cross-section where, in the limit of low Re and large curvature radius R_c, fluid motion approaches that in the idealized plane square enclosure. As for the parallelepiped configuration, with increasing Re centrifugal instabilities trigger Goertler vortices that eventually become unsteady and transition to turbulence. However, the absence of end wall effects renders the toroid configuration a

more general fundamental paradigm than its parallelepiped predecessor.

EARLIER WORK

Numerical calculations of the 2D wall-driven flow in a plane rectangular enclosure have been performed by, for example, Ghia et al. (1982), Iwatsu et al. (1989, 1990) and Nishida and Satofuka (1992). Corresponding 3D calculations of the parallelepiped geometry have been performed by Koseff et al. (1983), Freitas et al. (1985), Kim and Moin (1985), Freitas and Street (1988), and Iwatsu et al. (1989, 1990). Experimental investigations of the parallelepiped geometry include the pioneering studies performed by Koseff and Street (1984a, b, c), and later by Prasad and Koseff (1989) and Aidun et al. (1991). The stability of the 2D base flow to longitudinal disturbances in an infinitely long parallelepiped has been investigated numerically by Ramanan and Homsy (1994), Ding and Kawahara (1998, 1999) and , more recently, by Albensoeder et al. (2001). By means of linear stability analysis and experiments, the latter show the dependence of the instabilities observed on the enclosure cross-section dimensions. For parallelepipeds of cross-section equal to or close to square, they conclude that the steady 2D flow destabilizes to a steady 3D flow of dimensionless wavenumber κ ($\equiv 2\pi/(\lambda/D)$) = 15.43 for a critical Re = 786.3. They also find from their experiments that end wall effects can suppress instabilities in finite-length parallelepipeds.

The investigations performed in parallelepipeds reveal significant cross-stream motions in planes perpendicular to the main shear-driven recirculating flow. These motions are induced by: a) transverse pressure gradients arising at each of the two end walls; and, b) centrifugal instabilities responsible for Goertler vortices that arise above a critical value of the Reynolds number (or an equivalent Goertler number). The vortices appear as counter-rotating pairs periodically distributed in the longitudinal direction (x-direction in Fig. 1-b) and with their axes aligned with the main recirculating flow. (They have been referred to as Taylor-Goertler-like vortices in the literature but appear to share more in common with the centrifugal instability investigated by Goertler (1951) in curved boundary layers than the centrifugal instability investigated by Taylor (1923) in the space between concentric cylinders in relative rotation.)

The end wall pressure gradients in parallelepipeds fix the sense of rotation of the first vortex next to each wall. In turn, the end wall vortex fixes the sense of rotation of the Goertler vortex next to it and so on. Because the end wall pressure-gradient forces differ in magnitude from the centrifugal forces, and because of secondary instabilities, non-linear interactions among the vortices can induce time- and space-dependent variations among them as well as in their number. Although interesting, there is an unavoidable bias in the finite parallelepiped configuration that unnecessarily complicates both the physical understanding and the numerical calculation of 3D shear-driven enclosure flows.

A NEW SHEAR-DRIVEN ENCLOSURE FLOW PARADIGM

The end wall bias present in the finite parallelepiped geometry can be completely removed by turning the parallelepiped into a toroid. This is accomplished conceptually by curving the parallelepiped uniformly around a pair of parallel longitudinal walls and "dissolving" the end walls at the common plane where they meet to create a continuous, unobstructed toroid of square cross-section (Fig. 2-a). One of the flat walls of the toroid (the top wall in Fig. 2-a) is made to slide radially outwards (or inwards) with an axisymmetric velocity distribution in order to drive the flow in the toroid by viscous shearing. In addition to Re, the new quantity $\delta = D/R_c$ must be specified to characterize the fluid motion. Clearly, for values of $\delta \rightarrow 0$, the effects of geometrical curvature are rendered negligible, resulting in a flow configuration which: i) at sufficiently low Re rigorously approximates the 2D shear-driven flow in a plane square enclosure; ii) at sufficiently high Re will display the Goertler vortices observed in finite parallelepipeds, but *devoid* of end wall bias; and, iii) at even higher Re will undergo transition to turbulence. In this sense then, the shear-driven flow in a toroid represents a more general fundamental fluid mechanics paradigm than its predecessors.

Using the second order accurate (space and time) explicit CUTEFLOWS Navier-Stokes solver of Humphrey et al. (1995), Phinney and Humphrey (1996) and Sudarsan et al. (1998) have calculated the shear-driven flow in a toroid of square cross-section to investigate the effects of varying δ and Re on the flow. In particular, the latter show that above a critical value of Re, depending on the value of δ, the flow is rendered 3D and periodic in the circumferential direction by the appearance of pairs of Goertler vortices that can alternate their sense of rotation with time.

The present work explores the 3D, unsteady flow regimes in two shear-driven toroids of square cross-section. The study is part of an ongoing collaboration between JACH at the University of Virginia (UVA) and FG and JH at the University of Rovira i Virgili (URV). With reference to Fig. 2-a, Case 1 (the idealized case) consists of a toroid with $g/D = 0$, the top wall sliding radially outwards with axisymmetric, constant velocity U. With reference to Fig. 2-b, Case 2 (the experimental approximation to Case 1), $0 < g/D << 1$ and the flow is driven by the shearing action of the wall jet that expands radially outwards along the toroid top wall. For Case 1, calculations are performed for $\delta = 0.005$ with Re = 3200, and for $\delta = 0.25$ with Re = 2400. For Case 2, the Reynolds number is defined as $Re_g = U_g D/\nu$,

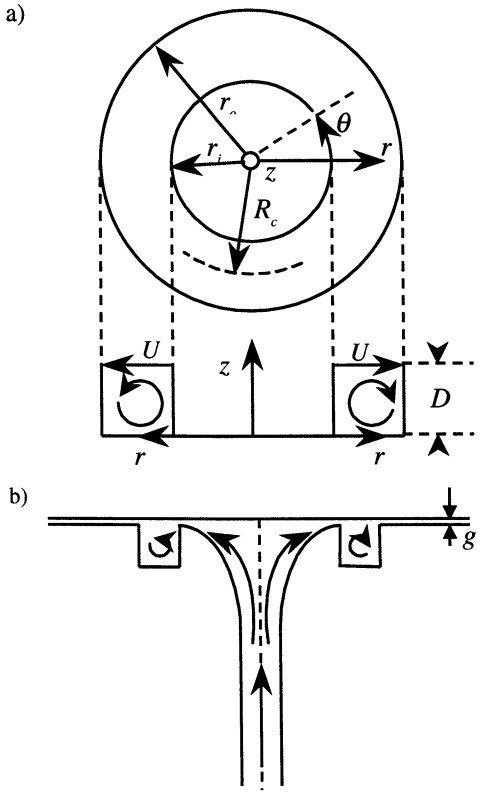

Figure 2. Experimental approximation (b, side view) of the shear-driven flow in an idealized toroid configuration (a, top view). In the experiment it is the shearing action of the fluid that drives the flow in the toroid. Note, $g << D$.

where U_g is the mean velocity of the fluid in the gap at the plane where it enters the toroid. For this case calculations are performed for $\delta = 0.51$ and $g/D = 0.04$ with $Re_g = 1143$, and visualization results are obtained for $\delta = 0.25$ and $g/D = 0.015$ with $Re_g = 5000$. The experiments for Case 2 are performed in an accurately machined plexiglass test section with $D = 0.05$ m and $R_c = 0.20$ m. The flow entrance section to the toroid is shaped like a trumpet of quarter-ellipse cross-section on which rests a vertically translatable flat top. This is fed by a constant head of water, metered and conditioned prior to entering the trumpet section. The flow in this section first decelerates slightly and then accelerates strongly as it approaches the toroid. Crushed mother of pearl illuminated by a plane light beam from a 5-mW He-Ne laser is used to visualize flow structures. See Cushner (2000) for further experimental details.

The original CUTEFLOWS code is used to calculate Case 1. For Case 2, a fourth order (space and time) version of the code, developed at URV, is employed. For Case 1, the length of the calculation domain in the circumferential direction consists of a sector of $\Delta\theta = 0.003$ rad for the case with $\delta = 0.005$ and $\Delta\theta = 0.157$ rad for the case with $\delta = 0.25$, these angles being estimated from scaling considerations based on experimental and numerical results in parallelepipeds. For Case 2, the calculation domain consists of the entire toroid. For Case 1 circumferentially periodic and symmetric boundary conditions are explored with the periodic yielding more realistic results. In both cases the no-slip condition is imposed for velocity at all surfaces in the toroid. For Case 2, the flow in the gap where it enters the toroid is fully developed Poiseuille flow. The flow leaving the toroid redevelops in a gap of equal g/D and length $l/D = 0.55$. For both Case 1 and 2 calculations are started from corresponding 2D (axisymmetric) solutions. For Case 1 it is necessary to seed the flow with weak, volume distributed, random disturbances to accelerate the appearance of the Goertler vortices. This was also the case in the shear-driven parallelepiped calculated by Kim and Moin (1985) but is counter to the findings of earlier linear stability analyses which show that the 2D flow in an infinitely long parallelepiped is unstable to infinitesimal disturbances. We attribute the need for artificial disturbances in Case 1 to numerical diffusion. In contrast, for Case 2, using the higher order scheme, such disturbances are not necessary and the vortices appear spontaneously. For both cases substantial grid refinement tests are performed culminating in (N_r, N_z, N_θ) grids of (50, 50, 30) for Case 1 and (72, 72, 192) for Case 2. (In particular, the new fourth order (space and time) version of CUTEFLOWS was shown to yield vortical flow structures with characteristics in excellent agreement with those obtained by Albensoeder et al. (2001), calculated here in a parallelepiped of square cross-section corresponding to Fig. 1-b with $L/D = 2$ and using periodic boundary conditions in the x direction; namely, we find $\kappa = 15.7$ at $Re = 850$.) For Case 1 with $\delta > 0$, the calculation time step was 10^{-3} s and for Case 2 it was less than 10^{-1} s. Typical calculation times for Case 2 on a dual processor Dell workstation (PWS620) are 9.67 hours for 100 seconds of numerical flow development.

RESULTS AND DISCUSSION

A brief summary of some main findings is provided here using Case 2 for illustration. (For Case 1 a digital movie is available.) Figures 3 and 4 show experimental visualizations of the flow (obtained at different times) in various z^*-θ and r^*-θ planes for $Re_g = 5000$, $\delta = 0.25$, and $g/D = 0.015$; $r^* \equiv (r-r_i)/(r_o-r_i)$ and $z^* \equiv z/D$. Although this condition corresponds to an unsteady flow regime, Goertler vortices of approximate wavenumber $\kappa = 12.5$ are clearly observed. At small values of z^* (near the toroid bottom wall), the vortices are radially aligned and fill the entire space between $r^* = 0$ and 1. With increasing z^* the vortices orient themselves axially and are especially prominent along the inner curved half of the toroid, $r^* < 0.5$. Calculated values of the instantaneous circumferential velocity component for Case 2 with $Re_g = 1143$, $\delta = 0.51$ and $g/D = 0.04$ are "visualized" using shades of gray ranging from

white to black in Fig. 5. These 3D results are in excellent qualitative agreement with the experimental observations in so far as the spacial distributions of the vortices is concerned. For the lower Re_g and larger δ calculated, however, flow unsteadiness is markedly reduced, and the wavenumber of the structures is $\kappa = 8.7$. (Note well: in a toroid κ ($\equiv 2\pi/(\lambda/D)$) = $(2\pi Rc/\lambda)\ \delta = N_{GP}\ \delta$ where N_{GP} is the total number of Goertler vortex pairs.)

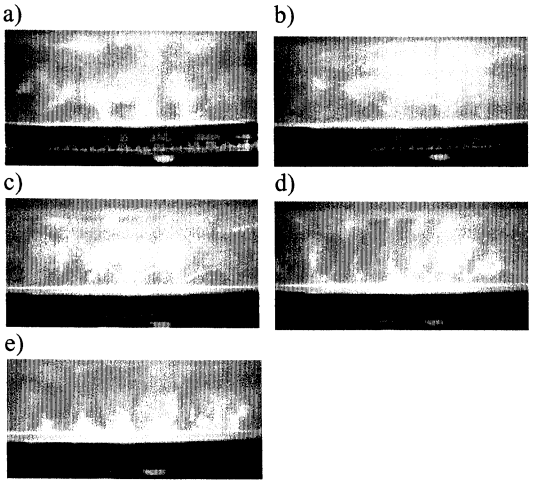

Figure 3. Visualization of the flow in a toroid with Re_g = 5000, $\delta = 0.25$ and $g/D = 0.015$. Pictures show views of z^*-θ planes as seen through the curved outer side wall of the toroid: (a) $r^* = 0.9$; (b) 0.7; (c) 0.5; (d) 0.3; and (e) 0.1.

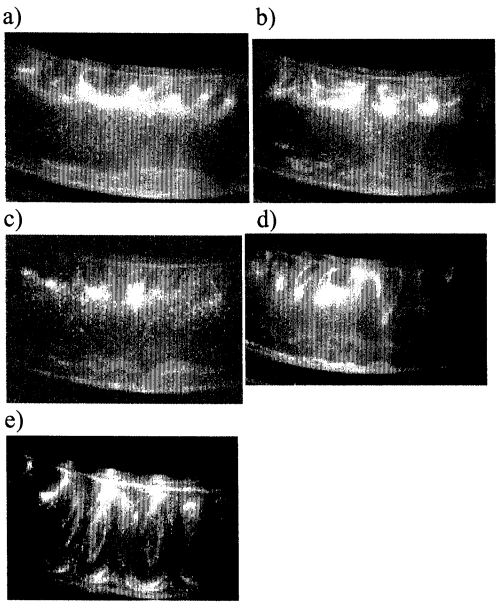

Figure 4. Visualization of the flow in a toroid with Re_g = 5000, $\delta = 0.25$ and $g/D = 0.015$. Pictures show views of r^*-θ planes as seen through the top wall of the toroid over a sector of 18 degrees: (a) $z^* = 0.9$; (b) 0.7; (c) 0.5; (d) 0.3; and (e) 0.1.

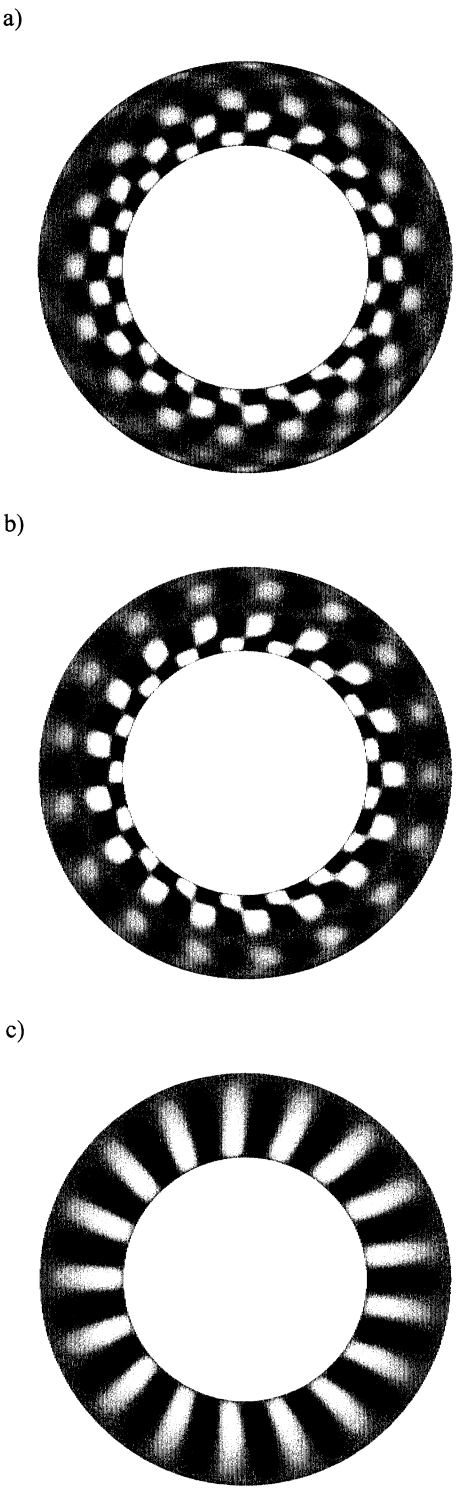

Figure 5. Instantaneous distributions of the calculated circumferential velocity component at $t^* = 779$ in r^*-θ planes of the toroid with $Re_g = 1143$, $\delta = 0.51$ and $g/D = 0.04$: (a) z^*=0.7; (b) 0.5 and (c) 0.1. Black and white areas denote regions of opposite velocity.

Figure 6 provides a calculated time record of the dimensionless circumferential velocity component ($u^*_\theta = u_\theta / U_g$) at $z^* = 0.5$, $r^* = 0.5$ and $\theta = 0.22\pi$ for the conditions of Fig. 5 The plots in Fig. 5 correspond to t^* ($\equiv tU_g/4D$) = 779 in the record. Although the magnitudes of the monitor velocity and its changes in Fig. 6 are very small, and while the flow has had a fairly large number of enclosure "turnovers" to develop, it appears to still be evolving. At the time of writing we have not yet concluded the calculations of these conditions. Therefore, we cannot say definitively that the flow dynamics continues to evolve towards a final, periodic state, or that it is actually orbiting within the basin of a strange attractor. Nevertheless, it is especially noteworthy that the entire flow in the toroid alternates between two states as a function of time. This is most clearly illustrated in the velocity vector plots presented for two times in the z^*-θ plane located at $r^* = 0.5$, in Fig.7. While the shape, size and number of the calculated structures are the same at both times, their location relative to a fixed circumferential reference location has been displaced by half a wavelength ($\lambda/2$). A similar observation has been made by Sudarsan et al. (1998) and we believe the phenomenom is asociated with a periodic coupling (via the shearing flow) between the tilting and stretching of θ-component of vorticity near the outer-radius wall of the toroid with that occuring at the inner-radius wall. However, further calculations and analysis are necessary to elucidate this.

Time averages of the results calculated for Case 1 with Re = 3200 and δ = 0.005 (not plotted here) show very good agreement with the Goertler structures and time-averaged velocity profiles obtained by Koseff and Street (1984a, c) in a parallelepiped with Re = 3300. For these conditions and for Re = 2400 with δ = 0.25, the flow is very unsteady and the Goertler vortices are observed to meander chaotically.

To conclude this section we comment on a basic difference between the toroid flows corresponding to Case 1 (Fig. 2-a) and Case 2 (Fig. 2-b). This has to do with the manner of fluid shearing. In Case 2, a

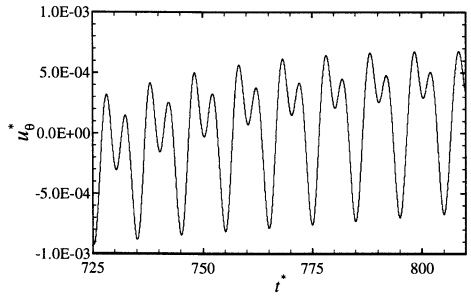

Figure 6. Time record of the dimensionless circumferential velocity component at $z^* = 0.5$, $r^* = 0.5$ and $\theta = 0.22\pi$ for the conditions of Fig. 5.

a)

b)

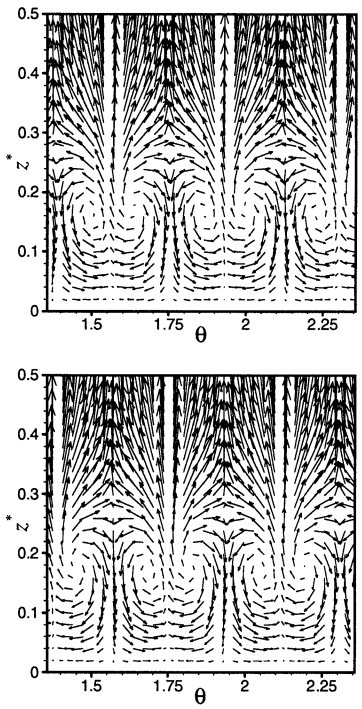

Figure 7. Instantaneous velocity vectors at times t^*=783.2 (a) and t^*=788.0 (b).in the lower half of the z^*-θ plane at $r^* = 0.5$ for the conditions of Fig. 5.

wall-jet boundary layer develops along the top wall of the enclosure resulting in a stagnation line along the outer curved wall of the toroid that falls below the exit gap. Preliminary tests show that, for otherwise identical conditions, the 2D to 3D transition occurs at lower value of Reynolds, and the number of Goertler vortices is less, in a toroid for Case 1 than for Case 2.

CONCLUSIONS

Because of the absence of end wall effects, the shear-driven flow in a toroid of square cross-section represents a more general fluid mechanics paradigm than its parallelepiped predecessor. In the limit $\delta \rightarrow 0$ and at sufficiently low Reynolds number, the flow in a toroid approximates the 2D flow in a plane enclosure. At sufficiently high Reynolds number, the flow in a toroid becomes 3D and, eventually, unsteady. We provide here some new flow field results, as well as the finding that, in a toroid, the wavenumber $\kappa = N_{GP}\,\delta$ is 12.5 for δ = 0.25 (Case 2, experiments) and 8.7 for δ = 0.51 (Case 2, calculations). Also, in close agreement with Albensoeder et al (2001), we find κ = 15.7 in an infinitely long parallelepiped. This suggests that the wavenumber κ decreases with increasing curvature ratio, δ. Further work is necessary to neatly establish the transition from 2D to 3D flow, the appearance of flow unsteadiness, the conditions leading to (and an

understanding of) the time-dependent alternating sense of rotation of the Goertler vortices and, ultimately, transition to turbulence as a function of the relevant geometrical and dynamical parameters. Radial accelerations and decelerations induced by geometrical curvature on the flow in a toroid render it especially rich in its physics. While this physics has yet to be explored in full depth, both experimentally and numerically, the new paradigm posed here serves as a challenging test case for computational fluid dynamic procedures aimed at solving complex 3D unsteady laminar and turbulent flows.

ACKNOWLEDGMENTS

JACH gratefully acknowledges support received from NSF (grant CTS9504390) for this study. Thanks go to G. Waltman at Bucknell University for the construction of the toroid test section. MA, JH and FG thank the "Dirección General de Investigación Científica y Técnica" (Spain), DGICYT project no. PB96-1011, and the "Programa de Grups de Recerca Consolidats de la Generalitat de Catalunya", CIRIT project no. 1998SGR-00102, for their support. We are sincerely grateful to R. Eichhorn (University of Houston) and J. Heinrich (University of Arizona) for enlightening discussions.

REFERENCES

Aidun, C.K., Triantafillopoulous, N.G. and Benson J.D (1991) "Global stability of lid driven cavity with throughflow: Flow visualization studies," *Phys. Fluids* A, **3**, 2081-2091.

Albensoeder, S., Kuhlmann, H.C. and Rath, H.J. (2001) "Three-dimensional centrifugal-flow instabilities in the lid-driven-cavity problem," *Phys. Fluids* A **13**, 121-135.

Cushner, J. (2000) "Experimental visualization of a shear-driven toroidal LDC flow," M.Sc. Thesis, College of Engineering, Bucknell University, Lewisburg, Pennsylvania.

Ding, Y. and Kawahara, M. (1998) "Linear stability of incompressible fluid flow in a cavity using finite element method," *Int. J. Numer. Methods. Fluids*, **27**, 139-157.

Ding, Y. and Kawahara, M. (1999) "Three-dimensional linear stability analysis of incompressible viscous flows using the finite element method," *Int. J. Numer. Methods. Fluids*, **31**, 451-.

Freitas, C.J. and Street, R.L. (1988) "Nonlinear transient phenomena in complex recirculating flow: A numerical investigation," *Int. J. Numer. Methods Fluids*, **8**, 769-802.

Freitas, C.J., Street, R.L., Findikakis, A.N. and Koseff, J.R. (1985) "Numerical simulation of three dimensional flow in a cavity," *Int. J. Numer. Methods Fluids*, **5**, 561-575.

Ghia,U., Ghia, K.N. and Shin, C.T. (1982) "High-Re solutions for incompressible flow using Navier-Stokes equations and a multigrid method'" *J. Comput. Phys.*, **48**, 387-411.

Goertler, H. (1951) "On the three-dimensional instability of laminar boundary layers on concave walls" NACA Technical Memorandum No. 1375.

Humphrey, J.A.C., Schuler, C.A. and Webster, D.R. (1995) "Unsteady laminar flow between a pair of disks corotating in a fixed cylindrical enclosure," *Phys. Fluids*, **7**, 1225-1240.

Iwatsu, R., Hyun, J.M. and Kuwahara, K. (1990) "Analyses of three dimensional flow calculations in a driven cavity," *Fluid Dynam. Research*, **6**, 91-102.

Iwatsu, R., Ishii, K., Kawamura, T., Kuwahara, K. and Hyun, J.M. (1989) "Numerical simulation of three-dimensional flow structure in a driven cavity," *Fluid Dynam. Research*, **5**, 173-189.

Kim, J. and Moin, P. (1985) "Application of fractional step method to incompressible Navier-Stokes equations," *J. Comput. Phys.*, **59**, 308-323.

Koseff, J.R. and Street, R.L. (1984a) "Visualization studies of a shear driven three dimensional recirculating flow," *J. Fluids Eng.* **106**, 21-29.

Koseff, J.R. and Street, R.L. (1984b) "On end wall effects in lid driven cavity flow," *J.Fluids Eng.*, **106**, 385-389.

Koseff, J.R. and Street, R.L. (1984c) "The lid driven cavity flow: a synthesis of qualitative and quantitative observations," *J. Fluids Eng.*, **106**, 390-398.

Koseff, J.R., Street, R.L., Gresho, P.M., Upson, C.D., Humphrey, J.A.C. and To, W.M. (1983) "A three dimensional lid driven cavity flow: experiment and simulation," Proceedings of the Third International Conference on Numerical Methods in Laminar and Turbulent Flow, Seattle, WA, 564-581.

Nishida, H. and Satofuka, N. (1992) "Higher order solutions of square driven cavity flow using variable-order multigrid method," *Int. J. Numer. Methods Fluids*, **34**, 637-653.

Phinney, L.M. and Humphrey, J.A.C. (1996) "Extension of the wall driven enclosure flow problem to toroidally shaped geometries of square cross-section," *J. Fluids Eng.*, **118**, 779-786.

Prasad, A.K. and Koseff, J.R. (1989) "Reynolds number and end-wall effects on a lid driven cavity flow," *Phys. Fluids* A, **1**, 208-218.

Ramanan, N., and Homsy, G.M. (1994) "Linear stability of lid driven cavity flow," *Phys. Fluids*, **6**, 2960-2701.

R. Sudarsan, J.A.C. Humphrey and J. Heinrich (1998) "Three-dimensional unsteady wall-driven flow in a toroid of square cross-section: a new CFD paradigm," Proceedings of the ASME FED Summer Meeting: Forum on Industrial and Environmental Applications of Fluid Mechanics June 21-25, Washington DC

Taylor, G.I. (1923) "Stability of a viscous liquid contained beween two rotating cylinders," Phil. Trans. Roy. Soc., **45**, 289-343.